



# Simulation study on sectional ventilation of long-distance high-temperature roadway in mine

Ping Huang<sup>1</sup> · Wei Huang<sup>2</sup> · Yongliang Zhang<sup>3,4</sup> · Shibin Tang<sup>5</sup>

Received: 2 June 2021 / Accepted: 7 July 2021 / Published online: 5 August 2021  
© Saudi Society for Geosciences 2021

## Abstract

In order to solve the thermal damage caused by the long-distance high-temperature roadway mining stage in the late stage of the 20th middle section of the Daliuhang gold mine, fluent software and Ventsim software were used to simulate the tunnel cooling model. Firstly, the idea of sectional ventilation and cooling in long-distance high-temperature roadway is put forward, and the mathematical model of sectional uniform ventilation is established according to the theory of fluid mechanics. Secondly, the Fluent software is used to simulate and test the mathematical model. Thirdly, the Ventsim software is used to optimize the mine ventilation system, and the sectional ventilation cooling design is carried out. Finally, the cooling effect of roadway with conventional forced ventilation and sectional ventilation is simulated, and the simulation results are analyzed. The results show that: in the 220-m-long roadway in the late mining stage of the 20th middle section, the cooling effect of the roadway with sectional ventilation is about 15% higher than that of the conventional local ventilation. The cooling effect of the conventional forced ventilation near the working face of the 20th middle section is better than that of the sectional ventilation; when the return air distance exceeds 70m, the sectional ventilation cooling method is better than the conventional local ventilation cooling method.

**Keywords** Long-distance high-temperature roadway · Heat damage · Sectional ventilation and cooling · Sectional uniform ventilation

## Introduction

In China, the research of mine heat damage control started late and is still in the development stage. Due to the rapid

development of mining technology, a large number of mines have gradually turned to the stage of deep mining. In the process of deep mining, restricted by geological conditions and other special environment, the mine sometimes needs to carry out long-distance single-head mining operation. With the increase of ventilation distance, the problem of high-temperature heat damage is easy to occur in the return air stage of roadway (Cui et al., 2021; Feng, 2019; Zhang and Huang, 2020). China's "mine safety regulations" clearly stipulates that the air temperature of the working place of underground workers shall not exceed 28°C (Liu et al., 2019; Wang, 2011; Wang et al., 2019; Zhang et al., 2019; Zhang and Li, 2020; Zhang and Zhang, 2021). When the temperature exceeds 28°C, cooling and protection measures must be taken (Wu, 2019). Therefore, it is of great significance to study the heat damage treatment of long-distance high-temperature roadway, and solving the high-temperature problem of mine is beneficial not only to the development of enterprises, but also to the promotion of the whole mining industry and even the national social development.

At present, scholars have done a lot of research on ventilation and cooling of high-temperature roadway in deep mine.

---

Responsible Editor: Keda Cai

---

This article is part of the Topical Collection on *Geodesy and Geodynamics of China*

---

✉ Yongliang Zhang  
zhyoliang@163.com

<sup>1</sup> School of Environment and Safety Engineering, Fuzhou University, Fuzhou 350108, China

<sup>2</sup> Straits Institute, Minjiang University, Fuzhou 350121, China

<sup>3</sup> Key Laboratory of Ministry of Education for Efficient Mining and Safety of Metal Mines, University of Science and Technology Beijing, Beijing 100083, China

<sup>4</sup> School of Mechanical and Automotive Engineering, Qingdao University of Technology, Qingdao 266520, China

<sup>5</sup> School of Civil Engineering, Dalian University of Technology, Dalian 116024, China

Wang et al. (2013), Zhang et al. (2020), Lin (2018), Wei et al., 2018, Yan (2018), and others put forward the heat exchange equation between air flow in metal mine and surrounding rock of roadway, and used the low-temperature surrounding rock in constant temperature zone to absorb the heat of air flow, precooling the air flow, so as to reduce the air temperature entering the working face. Luo et al. (2020) and Yin et al. (2014) adopted the combination of air compression refrigeration and air conditioning and double-layer heat insulation air duct to solve the problem of heat damage in high-temperature excavation of metal mines. Li (2019) used the cooling principle of air source heat pump to build a set of underground air source heat pump cooling system to study the cooling of deep well mining.

In view of this, combined with the theory of fluid mechanics, the author established a piecewise uniform ventilation cooling model by using static pressure recovery method, and simulated and tested the model by using Fluent software (Qu et al., 2004; Tao et al., 2012; Zhang et al., 2021). Aiming at the long-distance roadway operation in Daliuhang gold mine in the late mining period, the design of sectional ventilation and cooling is carried out, and the cooling effect is simulated by using Ventsim software.

## Engineering background

The mining method of Yankou mining area in Daliuhang gold mine is a single-ended roadway mining. The ventilation system mainly uses the new well 958 as the air inlet shaft, blind well 568, and well 568 as the air return shaft. The whole mine adopts mechanical extraction ventilation, and the local working face adopts mechanical pressure ventilation. The main air intake shaft is well 958 which is directly connected to the surface. Fresh air flows into the shaft from well 958, enters the cleaning face through the middle roadway, and the waste air is discharged to the surface through the return air roadway, pedestrian ventilation shaft, blind well 568, and finally well 568. The specific ventilation route is well 958 to middle roadway to blind well 568 to -355m middle roadway to well 568. At present, the mine has nearly entered deep mining, and the situation of high temperature and high humidity is serious. The simplified diagram of ventilation route is shown in Figure 1.

According to the underground temperature monitoring, the temperature at the entrance of the 20th middle roadway has reached 30°C, and the temperature at the working face about 90m away from the entrance of the roadway has also reached 32°C. The high-temperature environment in the roadway has seriously affected the production operation, and seriously exceeded the maximum temperature of 28°C specified by the National Safety and Health Standards for Underground Operation. Therefore, it is necessary to optimize the existing

ventilation system and take measures to control the underground heat damage (Trujillo-Vela et al., 2019).

## Theoretical analysis of sectional ventilation cooling

### Mathematical model of sectional uniform ventilation

The sectional uniform ventilation model is an equal section uniform supply air duct with different sizes of air leakage ducts on the side of the air duct, and its end is open, as shown in Figure 2. The air leakage ducts have the same spacing, the length of the air duct is  $l$ , the sectional area is  $A$ , the air inlet air volume of the air duct is  $Q$ , and the air volume of each air leakage duct is  $Q_0$ . The size of the air leakage duct along the length of the duct is changed to ensure uniform air supply. Based on extensive field testing, in this paper, the static pressure method is used to establish the mathematical model of sectional uniform ventilation.

Number the air leakage duct from the end of the duct to the inlet. When the main air duct carries out uniform air supply, the sectional area of no.  $i+1$  air leakage duct is as follows:

$$S_{i+1} = \frac{Q_0}{v_{i+1}} \quad (1)$$

where  $S_{i+1}$  is the sectional area of no.  $i+1$  air leakage duct,  $m^2$ ;  $Q_0$  is the air volume of each air leakage duct,  $m^3$ ;  $v_{i+1}$  is the outlet wind speed of no.  $i+1$  air leakage duct,  $m/s$ .

$$v_{i+1} = \kappa \sqrt{\frac{2}{\rho} p_{i+1}} \quad (2)$$

where  $\kappa$  is the flow coefficient of air leakage duct,  $\kappa = \chi\varphi$ ;  $\chi$  is the shrinkage coefficient, in the orifice outflow,  $\chi$  is 0.60~0.64, in the outflow of nozzle,  $\chi$  is 1;  $\varphi$  is the velocity coefficient, numerical value is 0.97~0.98;  $\rho$  is the air density,  $kg/m^3$ ;  $p_{i+1}$  is the air static pressure of main air duct at no.  $i+1$  air leakage duct, Pa.

The energy equation is established at the center of nozzle no.  $i$  and nozzle no.  $i+1$ :

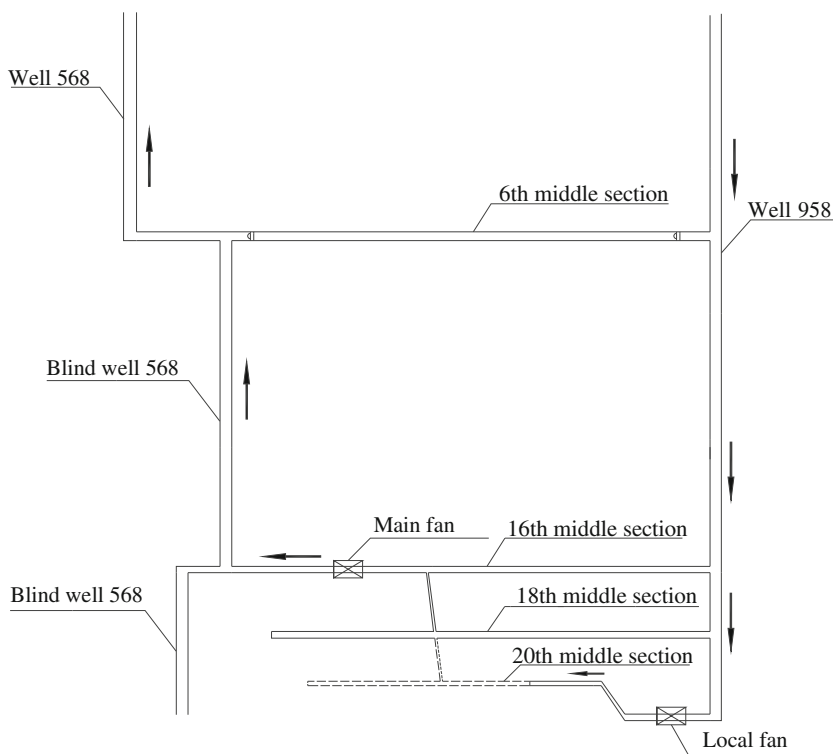
$$p_{i+1} = p_i + \Delta p_{mi} + Z_{i+1} - \frac{\rho}{2} (\omega_{i+1}^2 - \omega_i^2) \quad (3)$$

$$Z_{i+1} = \xi_{i+1} \cdot \frac{\rho}{2} \cdot \omega_{i+1}^2 \quad (4)$$

$$\Delta p_{mi} = \int_0^l \frac{\lambda}{d} \cdot \frac{\rho \omega_i^2}{2} dx = \frac{\lambda \rho}{2d(n+1)} \cdot \omega_i^2 = R_{mi} \cdot \frac{l}{n+1} \quad (5)$$

where  $\Delta p_{mi}$  is the resistance between two sections, Pa;  $Z_{i+1}$  is the local resistance at no.  $i+1$  air duct, Pa;  $\xi_{i+1}$  is the local resistance coefficient at no.  $i+1$  air duct;  $\omega_i$  is the air flow rate at no.  $i$  air duct,  $m/s$ ;  $\omega_{i+1}$  is the air flow rate at no.  $i+1$  air duct,

**Fig. 1** Simplified ventilation route



m/s;  $\lambda$  is the friction coefficient;  $R_{mi}$  is the frictional resistance per unit length, Pa;  $d$  is the equivalent diameter of air duct, m;  $l$  is the length of main air duct, m;  $n$  is the number of air leakage ducts.

According to Eqs. (1) and (2), the air static pressure at no.  $i$  air duct is:

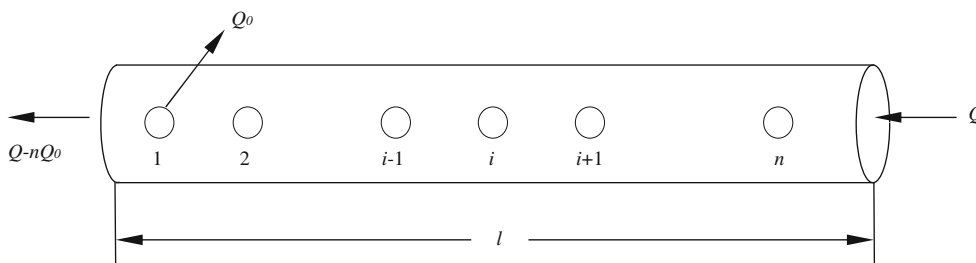
$$p_i = \frac{\rho v_i^2}{2\kappa^2} = \frac{\rho}{2\kappa^2} \cdot \frac{Q_0^2}{S_i^2} \tag{6}$$

Air flow rate at no.  $i$  air duct in air duct is:

$$\omega_i = \frac{Q_i}{A} = \frac{Q_0 - (n-i)Q_0}{A} \tag{7}$$

Solve Eqs. (1) to (7) to obtain the cross-sectional area of the air leakage duct:

**Fig. 2** Uniform air supply duct with equal cross section



$$S_{i+1} = \frac{1}{\sqrt{\frac{1}{S_i^2} + \frac{2l\kappa^2 R_{mi}}{Q_0^2(n+1)\rho} + \frac{\kappa^2}{Q_0^2} [(\xi_{i+1}-1)\omega_{i+1}^2 + \omega_i^2]}} \tag{8}$$

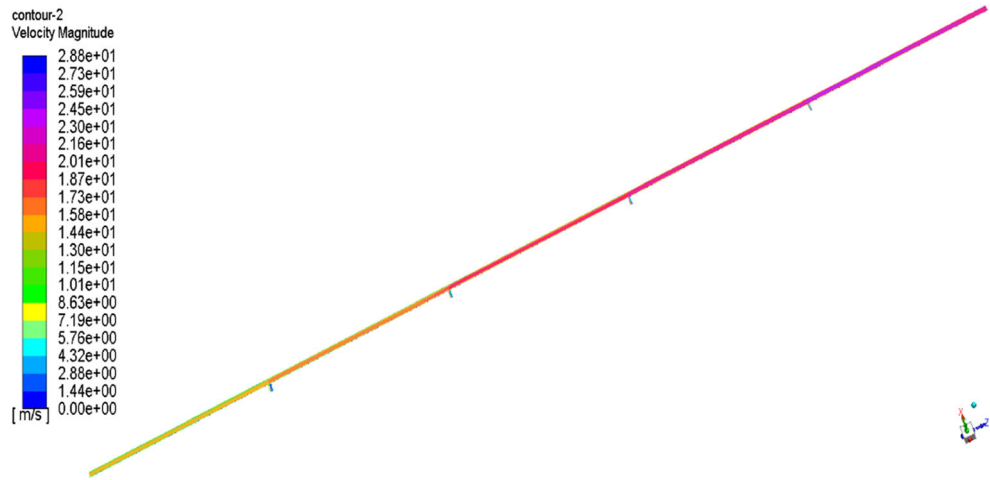
Among them, by substituting Eqs. (6) and (7) into Eq. (1), the formula of cross-sectional area of no. 1 air leakage duct is obtained:

$$S_1 = \frac{1}{\sqrt{\frac{2l\kappa^2 R_{m0}}{Q_0^2(n+1)\rho} + \frac{\kappa^2}{Q_0^2} [(\xi_1-1)\omega_1^2 + \omega_0^2]}} \tag{9}$$

**Velocity field test**

Based on the intuitive conclusion that the paper wants to draw; the Fluent software is used to simulate the air flow. The

**Fig. 3** Velocity field distribution of sectional uniform air supply duct



velocity field distribution cloud diagram of sectional uniform air supply duct is shown in Figure 3.

It can be seen from Figure 3 that the average wind speed in the main air duct gradually decreases from the inlet to the outlet (from right to left) due to the resistance in the air duct. And there is air leakage in the main air duct. When the air flow passes through the air leakage duct, the average air flow velocity in the main air duct decreases greatly in stages due to the joint action of small air volume and local resistance. In order to observe the pressure change of the wind speed in the air duct near the air leakage duct in detail, in the cloud diagram of the velocity field distribution of the  $Y=0.6\text{m}$  plane air duct, from left to right, make the local velocity field distribution cloud diagram of no. 1 to no. 4 air leakage duct in turn, as shown in Figs. 4, 5, 6, and 7.

As shown in Figures 4, 5, 6 and 7:

- (1) In the cloud diagram of velocity field distribution of  $Y=0.6\text{m}$  plane duct, under the effect of duct resistance, the wind speed in the main duct is high in the middle and low on both sides. Extended to the three-dimensional

model of air duct, the distribution of air velocity field can be expressed as the wind speed gradually decreases from the center of air duct to the inner wall.

- (2) When the air flows out through the air leakage duct, the wind speed on the outside (left) of the duct is greater than that on the inside (right). The main reason is the change of air flow cross section, resulting in the deceleration and pressurization area inside the air leakage duct, which leads to the separation of air boundary layer and the formation of eddy current inside the air leakage duct, and finally the low-speed area inside the air leakage duct.

For the convenience of analysis and observation, in the plane pressure field distribution nephogram of  $Y=0.6\text{m}$ , one wind speed measuring point is taken at each leakage duct outlet and main duct inlet and outlet, as shown in Figure 8. Because the wind speed of the plane where the measuring point is located is different, the wind speed of the point is not representative. Therefore, the average wind speed is taken as the plane wind speed for measurement at multiple points on the plane. So the wind speed of the measuring point is selected

**Fig. 4** Cloud map of local velocity field distribution of no. 1 air leakage duct

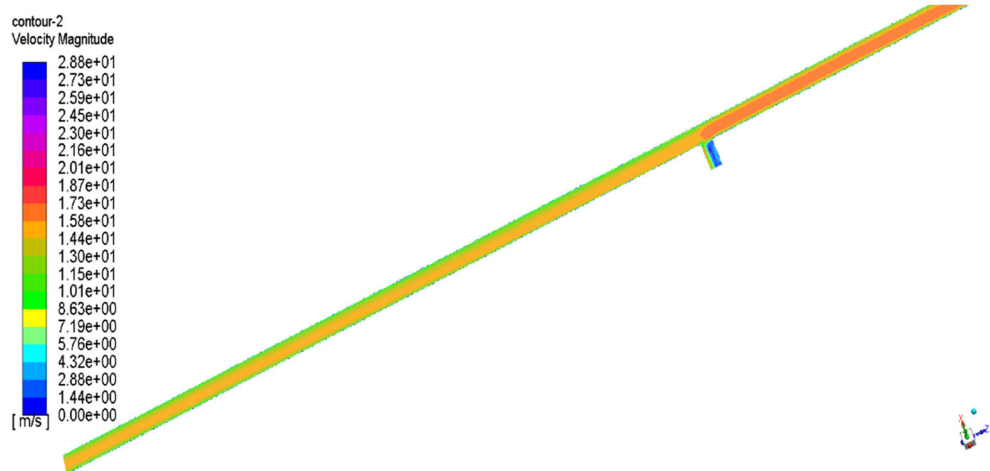
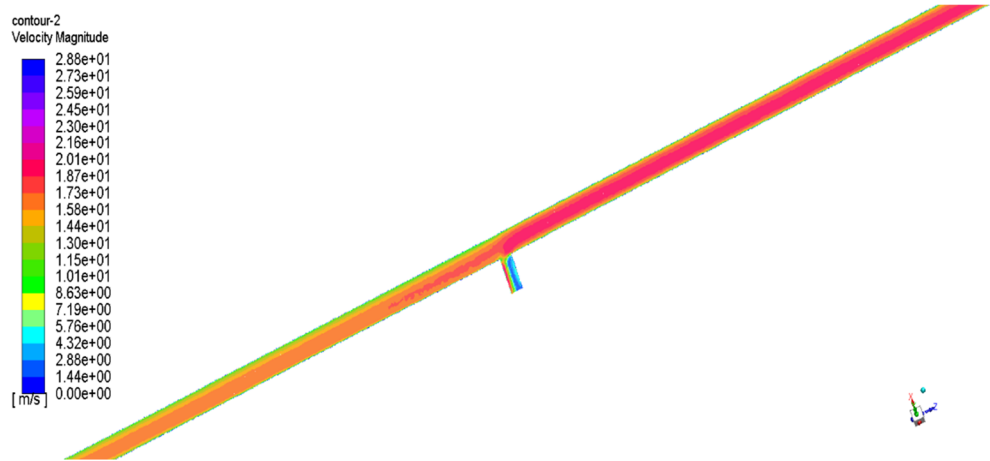


**Fig. 5** Cloud map of local velocity field distribution of no. 2 air leakage duct



as the average wind speed of the plane. And the average air volume of each measuring point is calculated according to Formula (7). According to the calculated average air volume, draw the broken line chart of sectional leakage air volume of uniform air supply duct, as shown in Figure 9.

It can be seen:

- (1) Measuring point 1 is the main air duct outlet, the air volume is about  $2\text{m}^3/\text{s}$ , measuring point 6 is the main air duct inlet, the air volume is  $4\text{m}^3/\text{s}$ , and the simulation results are consistent with the initial parameters of air flow.
- (2) The air volume values of measuring points 2–5 are the average air volume of no.1–4 air leakage ducts respectively. The fitting curve  $y = 0.499$  is obtained by fitting the data, which shows that the air volume values of each measuring point fluctuate around  $0.5\text{m}^3/\text{s}$ , that is, the average air output of each air leakage duct is about  $0.5\text{m}^3/\text{s}$ , which is consistent with the expected air distribution.
- (3) The simulation results of the mathematical model of sectional ventilation cooling are consistent with the

expected results, and the mathematical model is correct, which can be used to further study the effect of sectional ventilation cooling.

### Simulation of sectional ventilation cooling effect in Daliuhang gold mine

#### Optimization of ventilation system

##### Air volume calculation

According to the production regulations of metal mines, the total air demand of the mine is equal to the sum of the ventilation volume of each mining face, the independent ventilation chamber, and other ventilation volume, as well as the air leakage volume of the mine, and a certain safety reserve factor is set (Qu et al., 2004). According to the dust discharge calculation of the 20th middle section working face, the value of air volume is  $1.66\text{m}^3/\text{s}$ ; the minimum air volume of fine ore is  $0.68\text{m}^3/\text{s}$ , and the minimum air volume of installation

**Fig. 6** Cloud map of local velocity field distribution of no. 3 air leakage duct

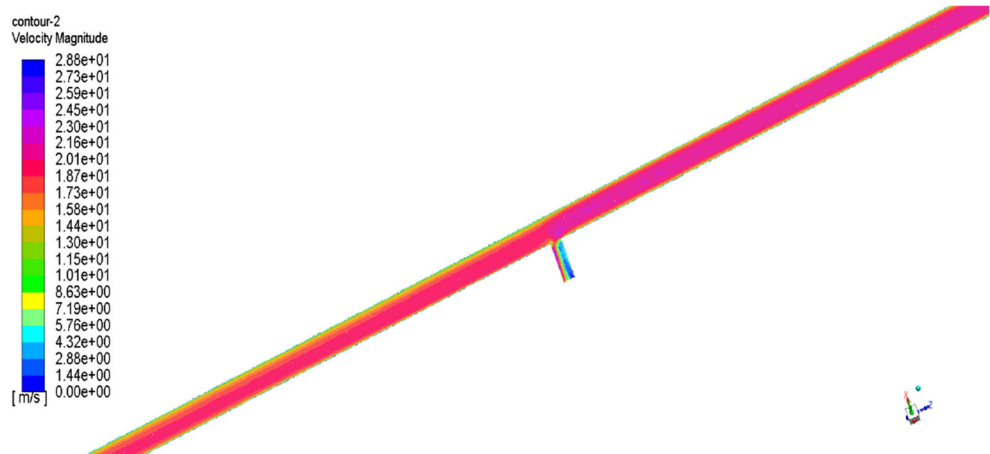
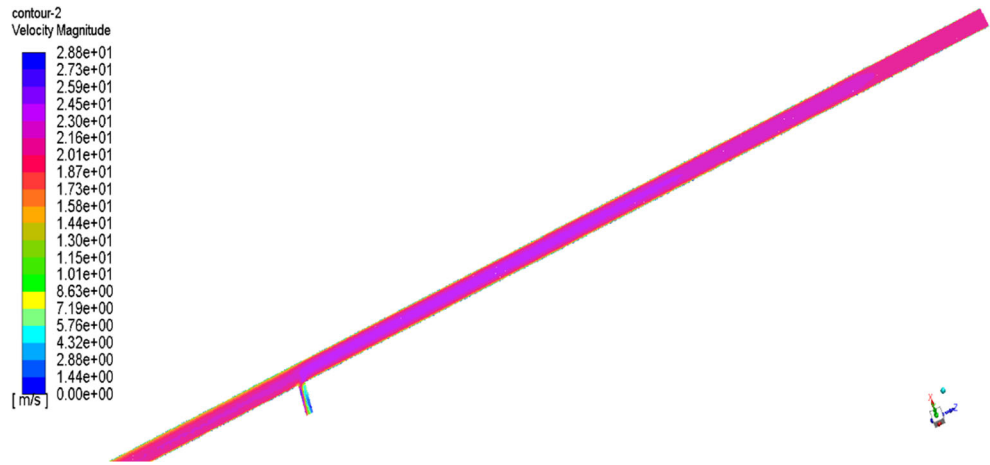


**Fig. 7** Cloud map of local velocity field distribution of no. 4 air leakage duct



chamber is  $0.77 \text{ m}^3/\text{s}$ . The minimum total air volume required by the ventilation system of the 20th middle section is  $3.11 \text{ m}^3/\text{s}$ . Considering a certain safety reserve factor, the safety reserve factor is taken as 1.25, and the total ventilation demand of the 20th middle section working face is finally determined as  $3.89 \text{ m}^3/\text{s}$ .

**Simulation of ventilation status**

Based on the field investigation in the mine, according to the layout of ventilation structures in the underground roadway, combined with the roadway model and ventilation parameters, the three-dimensional model of ventilation system is established by using Ventsim software, and the ventilation status is simulated, as shown in Figure 10.

According to the simulation of ventilation system in Yankou mining area in Figure 10, it can be seen that:

- (1) In well 958, the temperature of air flow is affected by geothermal, and increases with the increase of depth. The temperature increases from  $23.4^\circ\text{C}$  in the 6th middle section to  $26.6^\circ\text{C}$  in the 16th middle section.
- (2) In the air flow return stage from the middle section of the 16th to the blind well 568, the surrounding rock of the roadway is exposed for a long time, and the surrounding rock has a large heat-regulating ring. The surrounding rock temperature decreases with the decrease of depth. During the heat exchange between the wind flow and the surrounding rock, the heat flows to the surrounding rock,

- so there is a phenomenon of the decrease of the air temperature in the return wind stage.
- (3) Because the mining depth of the 20th middle section has reached  $-893.8\text{m}$ , the original rock temperature of the roadway is as high as  $39.2^\circ\text{C}$ , and the exposed surrounding rock is as high as  $32^\circ\text{C}$ , which leads to the temperature of the working face reaching  $32.8^\circ\text{C}$ , seriously exceeding the operation safety standard.
- (4) The air volume of the 20th middle section is only  $3.5 \text{ m}^3/\text{s}$ , which cannot meet the air demand of the working face.
- (5) The measured air volume data showed that the difference between the inlet air volume and the return air volume was  $2.3 \text{ m}^3/\text{s}$ , and there was air leakage in the ventilation system.

**Sectional ventilation design**

In the design, the 227-m-long roadway is cooled by 6 sections, that is, 5 air leakage ducts (every 36m) are set on the 220-m-long main duct (the outlet of the duct is 7m away from the working face). According to the conventional local ventilation cooling simulation, the air volume of the two local fans is  $6.3 \text{ m}^3/\text{s}$ . In order to ensure the air volume demand of about  $3.9 \text{ m}^3/\text{s}$  in the working face, the total air leakage volume is  $2.40 \text{ m}^3/\text{s}$ , and the air leakage volume of each air leakage duct is  $0.48 \text{ m}^3/\text{s}$ . According to the mathematical model of sectional ventilation, the sectional area of each air leakage duct is calculated:

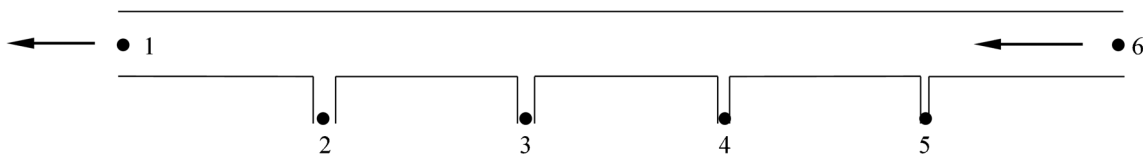


**Fig. 8** Distribution of measuring points of air duct on  $Y=0.6\text{m}$  plane

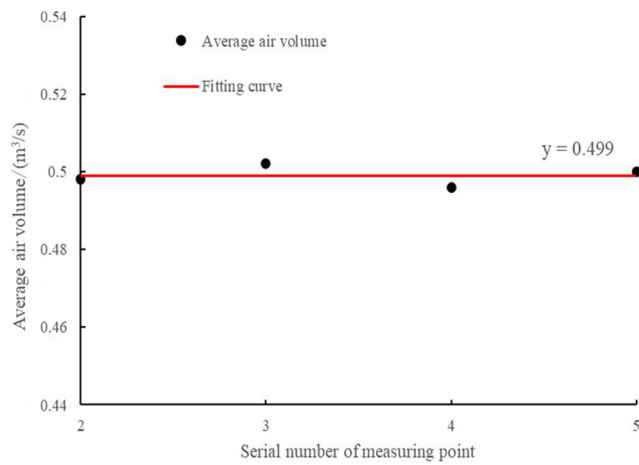


Fig. 9 Curve of air leakage volume of air duct section

$$S_1 = \frac{1}{\sqrt{\frac{2 \times 220 \times 0.9^2}{0.48^2 \times 6 \times 1.2} \times 26 + \frac{0.9^2 [(0.04-1) \times 43.8^2 + 39^2]}{0.48^2}}} = 0.0150\text{m}^2$$

$$S_2 = \frac{1}{\sqrt{\frac{1}{0.015^2} + \frac{2 \times 220 \times 0.9^2}{0.48^2 \times 6 \times 1.2} \times 49 + \frac{0.9^2 [(0.06-1) \times 48.6^2 + 43.8^2]}{0.48^2}}} = 0.0085\text{m}^2$$

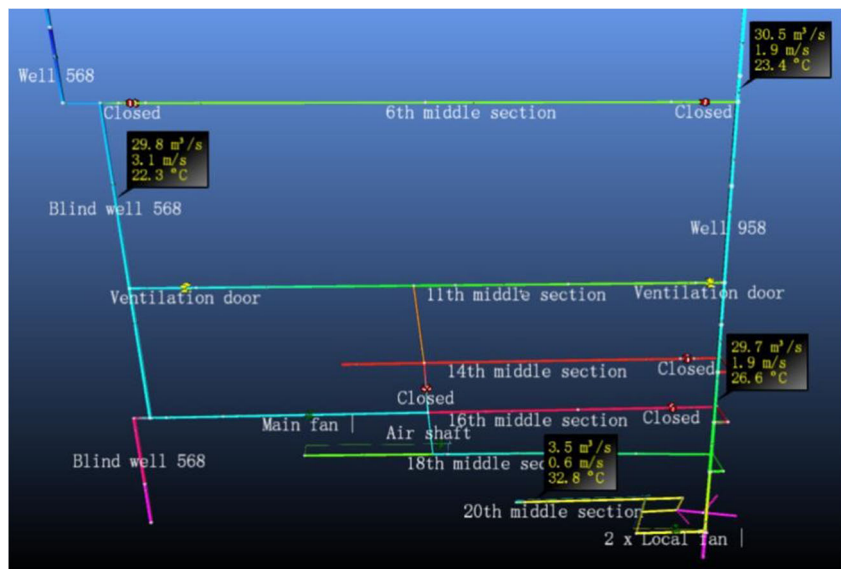
$$S_3 = \frac{1}{\sqrt{\frac{1}{0.0085^2} + \frac{2 \times 220 \times 0.9^2}{0.48^2 \times 6 \times 1.2} \times 50 + \frac{0.9^2 [(0.07-1) \times 53.4^2 + 48.6^2]}{0.48^2}}} = 0.0065\text{m}^2$$

$$S_4 = \frac{1}{\sqrt{\frac{1}{0.0065^2} + \frac{2 \times 220 \times 0.9^2}{0.48^2 \times 6 \times 1.2} \times 70 + \frac{0.9^2 [(0.08-1) \times 58.2^2 + 53.4^2]}{0.48^2}}} = 0.0052\text{m}^2$$

$$S_5 = \frac{1}{\sqrt{\frac{1}{0.0052^2} + \frac{2 \times 220 \times 0.9^2}{0.48^2 \times 6 \times 1.2} \times 73 + \frac{0.9^2 [(0.09-1) \times 63^2 + 58.2^2]}{0.48^2}}} = 0.0044\text{m}^2$$

The diameter of each air leakage duct is:  $d_1 = 0.138\text{m}; d_2 = 0.118\text{m}; d_3 = 0.114\text{m}; d_4 = 0.104\text{m}; d_5 = 0.102\text{m}$ .

Fig. 10 Simulation results of ventilation system status



### Simulation of cooling effect of sectional ventilation

In order to provide reference for future mining work, the application effect of ventilation and cooling design in the late stage of the 20th middle mining is simulated by using Ventsim software, as shown in Figure 11.

It can be seen from Figure 11 that the air flow simulation results of the sectional ventilation cooling design in the 20th middle section show that the air volume of the main air duct is  $6.3\text{m}^3/\text{s}$ , the air volume of the working face is  $3.9\text{m}^3/\text{s}$ , and the air volume of each leakage air duct is about  $0.5\text{m}^3/\text{s}$ . The simulation results are basically consistent with the expected results. The results show that the air flow and air volume distribution of the tunnel section ventilation and cooling design in the 20th section based on the section ventilation mathematical model are in line with the expectation, which can be used to conduct thermal simulation for the subsequent section ventilation and cooling design and analyze the cooling effect.

Thermal simulation is carried out for the ventilation and cooling design of the 20th middle section, and the simulation results are shown in Figure 12.

According to the simulation results of conventional local ventilation and sectional ventilation, the temperature change curve of the 20th middle section is drawn, as shown in Figure 13.

It can be seen from the above figure that the cooling effect of conventional local ventilation is better than that of sectional ventilation near the 20th middle section working face. With the increase of return air distance, the air flow and surrounding rock of roadway continue to exchange heat. The initial temperature of return air flow in roadway with conventional local ventilation cooling method is low, the temperature difference between surrounding rock of air flow is large, and the air flow temperature rises rapidly, however, the initial temperature of return air is higher, the temperature difference between

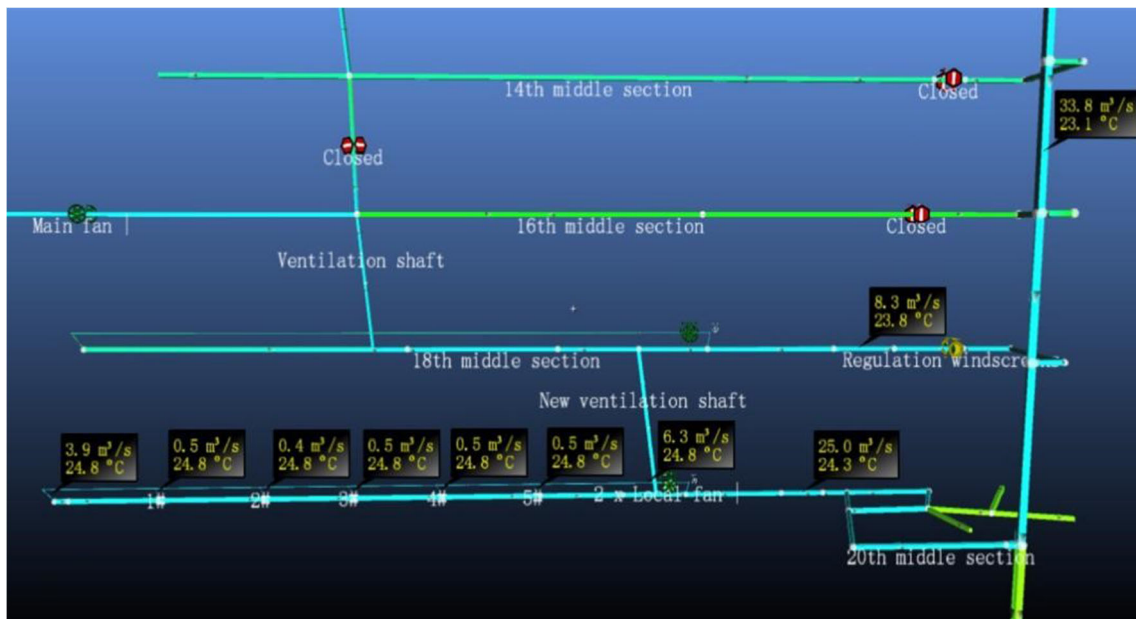


Fig. 11 The simulation of the air flow in the 20th middle section

surrounding rock is small, and the temperature rise of air flow is slow by adopting the method of sectional ventilation. In the cooling simulation of the 20th middle roadway, the sectional ventilation cooling method is better than the conventional local ventilation cooling method when the return air distance exceeds 70m. The effective cooling length of conventional local ventilation is 75m, accounting for about 34% of the total roadway. The effective cooling length of sectional ventilation is 108m, accounting for about 49% of the total roadway. Therefore, in the late stage of the 20th middle section mining, the cooling effect of the roadway with sectional ventilation is about 15% higher than that of the conventional local ventilation.

### Conclusion

- (1) Fluent software is used to simulate and test the mathematical model of sectional uniform air supply. The wind pressure and speed in the simulation results are basically consistent with the expected results. The model is correct and can be used for sectional ventilation and cooling design.
- (2) Aiming at the problem of heat damage in the late mining period of the 20th middle section of Daluohang gold mine, the subsection ventilation cooling method based on the subsection uniform air supply mathematical model was used to study the cooling effect, and the

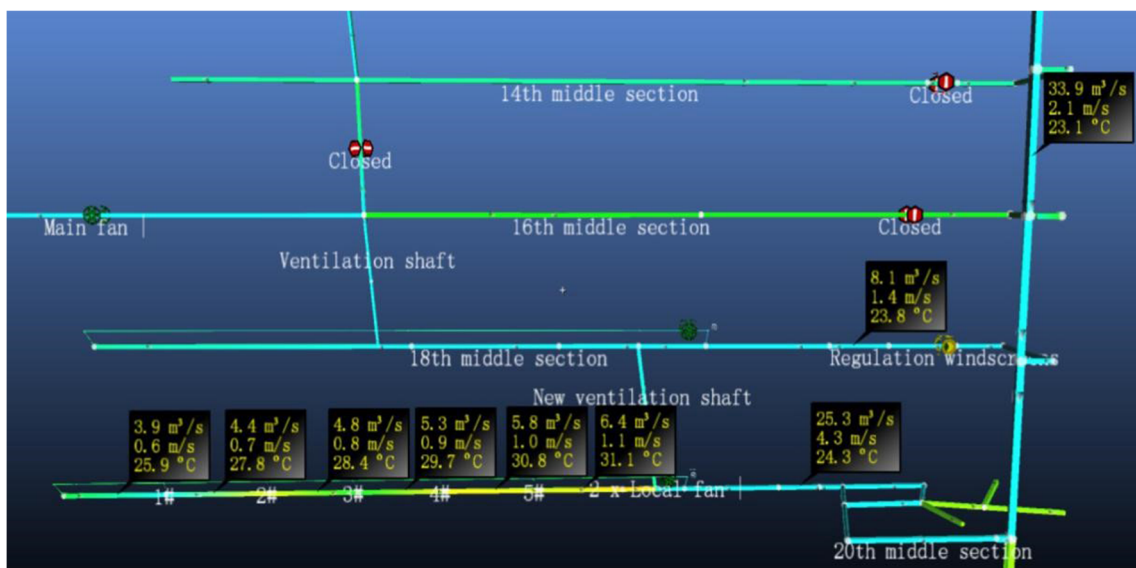
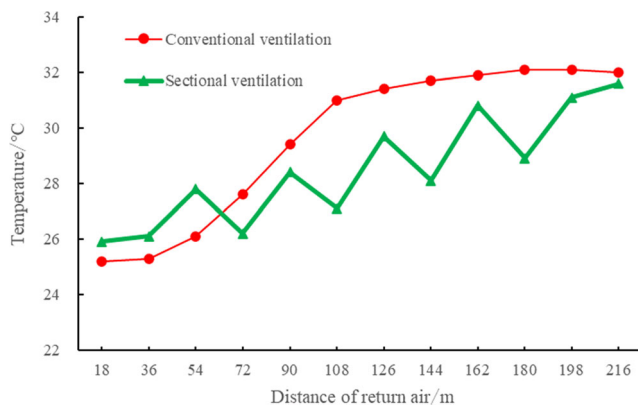


Fig. 12 Thermal simulation of sectional ventilation and cooling in the 20th middle section





**Fig. 13** Temperature change curve of the 20th middle section

application effect was simulated by Ventsim software, and the results show that in the 220-m-long roadway in the late stage of the 20th middle mining, the cooling effect of the roadway with sectional ventilation is about 15% higher than that of the conventional local ventilation.

- (3) In the cooling simulation of the 20th middle section roadway, the cooling effect of the conventional local ventilation is better than that of the sectional ventilation near the 20th middle section working face; when the return air distance exceeds 70m, the sectional ventilation cooling method is better than the conventional local ventilation cooling method.

**Funding** This work was supported by the Acknowledgements Financial support is provided by the National Science Foundation of China (51874187); Outstanding Youth Innovation Team Project in Shandong Colleges and Universities (2019KJH008); and Efficient Mining and Safety of Metal Mines Open Fund of Key Laboratory of Ministry Of Education (ustbmslab201802).

## Declarations

**Conflict of interest** The authors declare that they have no competing interests.

## References

Cui YY, Li K, Mei GD et al (2021) Research progress of analysis and control technology of heat stress in deep mine. *Nonferrous Metals (Mining Section)* 73(02):128–134

- Feng W (2019) Virtual display system of geological body based on key algorithms of three-dimensional modelling. *Earth Sci Res J* 23:185–189
- NN Li (2019) Study on cooling method and numerical simulation of air source heat pump in mine. *China University of mining and technology*
- Lin ZB (2018) Study on the application of wind bank to solve the problem of long distance roadway driving and ventilation. *World Nonferrous Metals* 03:231–232
- Liu YJ, Li M, Cao YJ et al (2019) Development of local cooling equipment for deep mines. *Modern Mining* 35(06):177–181
- Luo YD, Wang HN, Zhang YB (2020) Research and application of cooling technology in roadway driving in the mine at high temperature. *Nonferrous Metals Sci Eng* 11(01):85–91
- Qu F, Liu KG, Li YY et al (2004) Error analysis of measuring mine ventilation resistance by barometer base point method and selection of base point position. *Saf Coal Mines* 06:10–12
- Tao SY, Xiong ZM, Cheng Z et al (2012) Study on the optimization of ventilation system of metal mine. *Mining Res Dev* 32(02):58–60 +83
- Trujillo-Vela MG, Escobar-Vargas JA, Ramos-Canon AM (2019) A spectral multidomain penalty method solver for the numerical simulation of granular avalanches. *Earth Sci Res J* 23:317–329
- Wang YL (2011) Design of movable regional cooling system for mine. *Refrigeration* 11(06):44–48
- Wang YM, Chen YH, Jia MT (2013) Technology of ventilation and pre-cooling for deep high-temperature roadway of metal mines. *Metal Mine* 02:143–146
- Wang B, Liu S, Jin B, Qiu W (2019) Fine imaging by using advanced detection of reflected waves in underground coal mine. *Earth Sci Res J* 23:93–99
- Wei C, Chu ZX, Zhang P et al (2018) Heat and moisture source distribution determination and analysis of long distance excavation roadway. *Saf Coal Mines* 49(01):202–205 +209
- Wu WZ (2019) Numerical simulation of local ventilation air reservoir size for long distance tunneling face. *Coal Technol* 38(09):94–97
- Yan HY (2018) Analysis of water cooling technology by gravity for mining refrigeration unit. *Coal Eng* 50(12):79–81
- Yin CS, Li YC, Li XB (2014) Program research on ventilation and dust removal system in single-head and long-distance excavation of roadway. *Coal Technol* 33(11):54–56
- Zhang YL, Huang P (2020) Influence of mine shallow roadway on air-flow temperature. *Arab J Geosci* 13:12
- Zhang YL, Li M (2020) Research on flow and heat transfer characteristics of heat transfer surface of trapezoidal duct. *Heat Mass Transf* 56:1475–1486
- Zhang XL, Zhang YL (2021) Experimental study on enhanced heat transfer and flow performance of magnetic nanofluids under alternating magnetic field. *Int J Therm Sci* 164(106897):1–9
- Zhang YL, Zhang XL, Li M, Liu Z (2019) Research on heat transfer enhancement and flow characteristic of heat exchange surface in cosine style runner. *Heat Mass Transf* 55(11):3117–3131
- Zhang XL, Zhang YL, Lu CG (2020) Flow and noise characteristics of centrifugal fan in low pressure environment. *Processes* 985:1–12
- Zhang B, Xue PY, Liu L et al (2021) Exploration on the method of ore deposit-geothermal energy synergetic mining in deep backfill mines. *J China Coal Soc* 3:1–14